Journal of Porphyrins and Phthalocyanines
J. Porphyrins Phthalocyanines 2022; **26**: 533–541
DOI: 10.1142/S1088424622500018

Published at https://www.worldscinet.com/jpp/

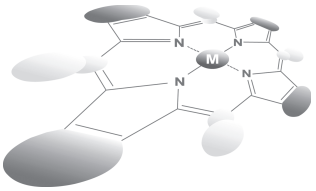

Combination of tetrapyridylporphyrins and arene ruthenium(II) complexes to treat synovial sarcoma by photodynamic therapy

Manuel Gallardo-Villagrán[a,c], Lucie Paulus[a], Yves Champavier[a,b], David Yannick Leger[a]*, Bruno Therrien[c]* and Bertrand Liagre[a]*

[a] *Laboratoire PEIRENE, Faculté de Pharmacie, Université de Limoges, EA 7500, F-87025 Limoges, France*
[b] *BISCEm, NMR platform, Centre de Biologie et de Recherche en Santé (CBRS), Limoges, France*
[c] *Institut de Chimie, Université de Neuchâtel, Avenue de Bellevaux 51, CH-2000 Neuchâtel, Switzerland*

Received 11 October 2021
Accepted 27 October 2021

POLYTHEA special issue

ABSTRACT: Four tetrapyridylporphyrin and four dipyridylporphyrin arene ruthenium complexes have been synthesized and characterized. In these complexes, the porphyrin core is either metal-free or occupied by zinc, and the arene ligand of the arene ruthenium units are either the standard methyl-isopropyl-benzene (*p*-cymene) or the less common phenylpropanol (PhPrOH) derivative. The porphyrin derivatives are coordinated to four arene ruthenium units or only two, in accordance with the number of pyridyl substituents at the periphery of the porphyrins, 5,10,15,20-tetra(4-pyridyl)-21H,23H-porphine (TPyP) and 5,15-diphenyl-10,20-di(pyridin-4-yl)porphyrin (DPhDPyP). All eight complexes were evaluated as anticancer agents on synovial sarcoma cells, in the presence and absence of light, suggesting that both the arene ligand and the porphyrin core substituent can play a crucial role in fine-tuning the photodynamic activity of such organometallic photosensitizers.

KEYWORDS: photodynamic therapy, porphyrins, arene ruthenium, synovial sarcoma.

INTRODUCTION

Could we cure cancer with light? The answer is yes we could, using photodynamic therapy (PDT). However, light must go hand in hand with oxygen and a chemical compound that acts as an intermediary between the other two. The energy from light can be absorbed and reused or transferred by substances that we know as photoactive compounds, chromophores or photosensitizers (PS). These substances reach a higher energy excited state as a consequence of their interaction with photons. During relaxation, the PS can interact with other molecules or substrates to transmit the absorbed energy. This is the principle on which PDT is based (Fig. 1). In PDT, the PS is irradiated at a certain wavelength (λ), reaching an excited singlet state. During relaxation to ground state, the PS can go through an intermediate excited triplet state and interact with O_2 (Fig. 2). This interaction can produce singlet oxygen ($^1O_2$) that in turn can give rise to radical oxygen species (ROS) [1–4]. The key to PDT is ROS production, since it could lead to oxidative stress and consequently to cell death [5, 6]. Moreover, ROS are tremendously reactive, so their lifetime lasts only a few nanoseconds [2, 7], which makes the cell death process specifically located to the irradiated area. For these reasons, PDT is considered non-invasive, and its use is increasingly widespread in the fight against cancer and other diseases.

Throughout recent decades, PDT has been one of the most fast-growing treatments against skin cancer [8, 9], acne [10, 11] and other skin diseases [12, 13]. The FDA have already approved the use of PDT in multiple pathologies like actinic keratosis, advanced cutaneous T-cell lymphoma, Barrett's esophagus, basal cell skin cancer, esophageal cancer, non-small cell lung cancer

*Correspondence to: David Yannick Leger, email: david.leger@unilim.fr, Bruno Therrien, email: bruno.therrien@unine.ch and Bertand Liagre, email: bertrand.liagre@unilim.fr

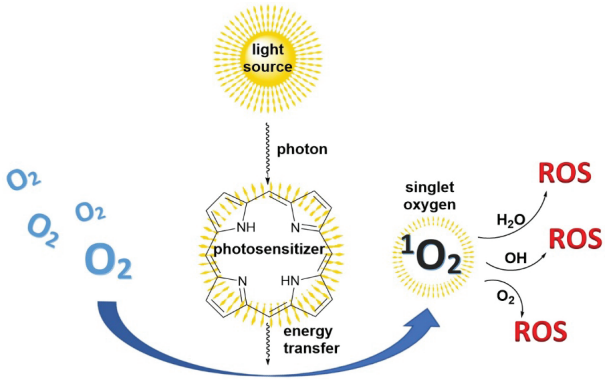

Fig. 1. Basic outline of the principles of PDT. The photosensitizer is excited by an external light source, transfers its energy to O_2, which is transformed into singlet oxygen, giving rise to reactive oxygen species (ROS).

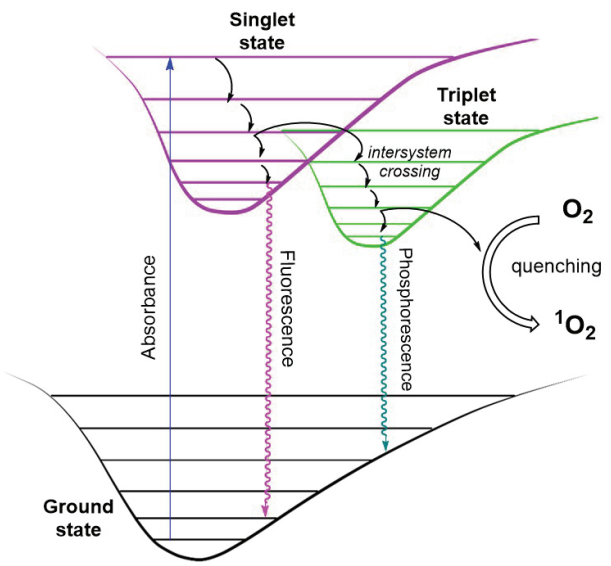

Fig. 2. Upon excitation to a singlet state, an electron can return directly to the ground state (fluorescence) or go through an intermediate triplet state (phosphorescence), where it can interact with O_2.

and squamous cell skin cancer. Furthermore, other types of cancer and more pathologies such as synovial sarcoma [14, 15], rheumatoid arthritis [16], bacterial infections [17, 18], are also under PDT investigations.

Synovial sarcoma is the fourth most common type of soft tissue cancer [19], representing approximately 10% of such cancers. It usually occurs in the surrounding area of large joints such as the synovial membrane, tendons, bursae or joint capsules. It is more common in men than women and in ages between 15 to 40 years old [20]. However, it is usually diagnosed late due to its slow progression, its benign appearance and the fact that it is often mistaken with pain due to trauma. The causes that give rise to this type of cancer are not yet fully understood [14]. The actual treatment involves invasive

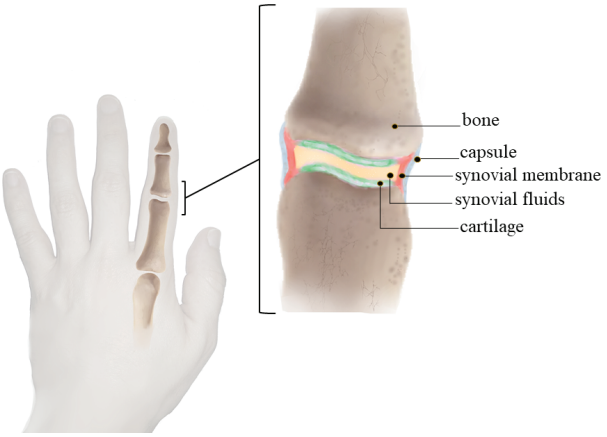

Fig. 3. Representation of the synovial tissue that connects the bones in the joints (only major tissues are represented).

surgery where tumoral tissues are removed [21]. Often, this is followed by radiotherapy and/or chemotherapy [22]. Evidently, this treatment entails a significant loss of soft tissue that can involve loss of mobility or add rigidity to the joint (Fig. 3). Therefore, minimizing the impact on healthy tissue can help to preserve better mobility in the joint and this is why PDT could play an important role, thanks to its minimal invasiveness and high precision.

However, PDT can likewise have some limitations, as a low solubility of PS, low concentration of oxygen in the target tissue or photosensitivity of the skin after treatment [23]. Many chromophores used in PDT show low solubility in biological media. This could lead to increase doses of PS to ensure optimal concentration in the target tissue, thus by increasing the dose of PS, side effects such as skin photosensitivity can appear. On the other hand, skin photosensitivity after PDT can be resolved using PS that require very low concentrations to be effective, in addition to the fact that the PSs can be totally inactive in the absence of light. A solution to increase solubility without increasing the dose is encapsulation of the PS in nanoparticles [24], coordination to peptides [25] or entrapment in lysosomes [26]. Also, it is possible to increase the solubility by designing PSs that incorporate hydrophilic substituents like sulfonate ($-SO_3H$) [27] or phosphonate ($-PO(OR)_2$) [28]. One more common solution is to use a solvent (other than water) in which the PS is soluble. However, it is necessary to take into account the toxicity of that solvent and the stability of the PS in this media, since some of these solvents are potential ligands and could degrade a drug before activation [29]. The inactivation or photoprotection of PS is another solution to limit photosensitivity. In this approach, the PS is transported in physiological medium and released selectively when necessary, thus reducing side effects [30–32].

Regarding the lack of oxygen, the accelerated growth of cancer cells generally leads to decreasing concentrations of O_2 [33, 34], which reduces the probability of giving rise to ROS. To resolve this inconvenience, it is

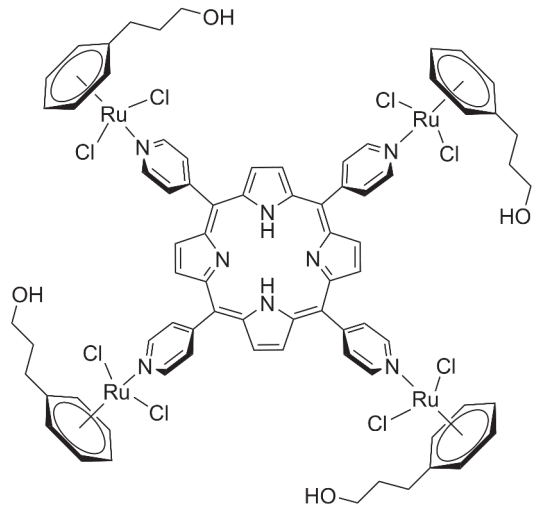

Fig. 4. Structure of a functionalized tetrapyridylporphyrin arene ruthenium complex.

possible to oxygenate the tumor tissue by hyperbaric oxygen therapy (HBO_2), prior to PDT [35].

Taking these aspects into account, we decided to design new PSs that increase the efficacy of PDT in synovial sarcoma based on the chromophore 5,10,15,20-tetra-(4-pyridyl)-21H,23H-porphine (TPyP). The TPyP is insoluble in water and poorly soluble in biological media. However, by coordination of arene ruthenium units to the pyridine substituents of TPyP (Fig. 4), solubility can be increased significantly. Moreover, these ruthenium complexes include arene ligands that have hydroxide groups (OH), that can potentially contribute to the presence of oxygen species, which can give rise to more $^1O_2$ and ultimately increase ROS production [36].

Ruthenium organometallic complexes are not new to PDT, since they have been used for years. The major reason behind that choice of metal is its oxidation state stability, being almost unreactive to air, water and O_2, unlike other metal-based compounds [37–43]. In addition, ruthenium has a high coordination number (6) and great facility to coordinate with ligands of complexed structures [37]. The arene ruthenium complexes could also improve the solubility in biological media [44]. Finally, ruthenium is less toxic than other metals such as platinum, a metal extensively used in metal-based drugs [45, 46].

In the present work, we show the synthesis and characterization of eight arene ruthenium complexes with tetrapyridylporphyrin or dipyridylporphyrin photosensitizers as a central ligand. For comparison, other derivatives incorporating different arene ligands, having two or four pyridyl groups, and with or without a metal in the core of the porphyrin have been synthesized and characterized. All new complexes were evaluated *in vitro*, in the presence and absence of light on synovial sarcoma cells.

RESULTS AND DISCUSSION

Synthesis and characterization of photosensitizers

The synthesis of the arene ruthenium PSs is carried out by a one step reaction (Scheme 1). The dinuclear arene ruthenium dimers (**d1** or **d2**), synthesized as reported in the literature [47, 48], are mixed and reacted with the corresponding porphyrin (Scheme 1). Dimer **d1** is widely used [49–52] since the publication in 1972 by Zelonka and Baird [47], while the dimer **d2** is a more recent analogue and its biological activity remains unexplored [48].

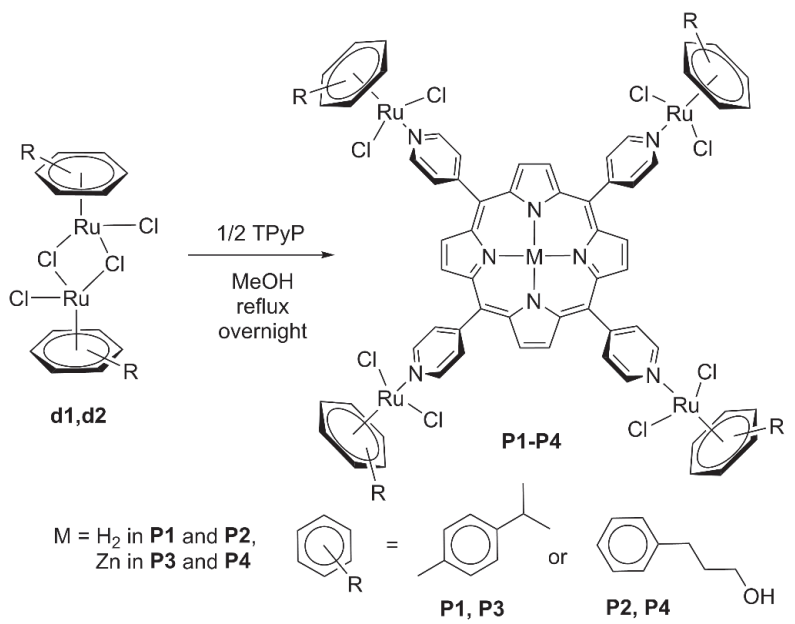

Scheme 1. Reactions of dimers **d1** or **d2** with TPyP or Zn-TPyP to form photosensitizers **P1**-**P4**.

As illustrated in Scheme 1, the reaction involves the breakage of the dimer into two monomers prior to the coordination of the porphyrin through a Ru–N(Py) bond. The reaction is carried out at reflux in methanol for at least 8 hr with a 2:1 molar ratio. Then, the suspension is filtered off and washed repeatedly with Et_2O, to obtain the desired tetranuclear complexes **P1**-**P4**. We had already reported the synthesis of **P1** ($[Ru_4(p\text{-cymene})_4(TPyP)Cl_8]$) [53]. However, new derivatives (with TPyP and Zn-TPyP) involving the dimer **d2**, giving rise to the photosensitizer **P2** ($[Ru_4(PhPrOH)_4(TPyP)Cl_8]$) and **P4** ($[Ru_4(PhPrOH)_4$-$(Zn\text{-}TPyP)Cl_8]$, and with dimer **d1** to give **P3** ($[Ru_4(p$-$cymene)_4(Zn\text{-}TPyP)Cl_8]$), have been also synthesized following the same methodology (see 'Experimental'). All compounds remain stable and unaltered at 4 °C for at least six months in the solid state. These compounds have acceptable solubility in DMSO and low solubility in other common solvents such as water, dichloromethane, chloroform, benzene, acetonitrile, acetone and ethanol. It should be noted that **P2** easily precipitates after minutes in DMSO. The recommended concentration of DMSO for *in vitro* tests is usually around 0.5%, although it depends on the cell line and the experimental conditions. According to the literature, 1% DMSO does not lead to toxicity in human myeloid leukemia and epithelia cancer [54]. On the other hand, in MDA-MB-231, MCF-7 and VNBRCA1 cell lines it is not recommended to use more than 0.6% of DMSO [55]. The maximum concentration used in our study has been 0.25% DMSO in the highest concentration of PS tested (5 μM). We have not observed any deleterious effect on synovial sarcoma cells that could be attributed to the presence of DMSO.

Similarly, we have synthesized and characterized four new derivatives, which are based on 5,15-diphenyl-10,20-di(pyridin-4-yl)porphyrin (DPhDPyP), giving rise to the corresponding photosensitizers **P5**-**P8** (Scheme 2). We have decided to explore the synthesis with this new porphyrin to study the influence of the number of ruthenium complexes coordinated to the porphyrin in terms of its efficacy in PDT, as well as the influence of the presence of phenyl groups in the porphyrinic unit. The experimental conditions are the same as those mentioned for TPyP but a 1:1 molar ratio is needed. Dimers **d1** and **d2** give rise to the photosensitizers **P5** ($[Ru_2(p\text{-cymene})_2(DPhDPyP)Cl_4]$) and **P6** ($[Ru_2(PhPrOH)_2(DPhDPyP)Cl_4]$) respectively, while **P7** ($[Ru_2(p\text{-cymene})_2(Zn\text{-}DPhDPyP)Cl_4]$) and **P8** ($[Ru_2(PhPrOH)_2(Zn\text{-}DPhDPyP)Cl_4]$) are synthesized from the Zn-porphyrin analogue, with **d1** and **d2** respectively. The yields are a bit lower than those observed with TPyP, between 51–67%. Like **P1**-**P4**, compounds **P5**-**P8** are soluble in DMSO. They also remain unaltered at 4 °C for at least 6 months in the solid state. All compounds are stable in DMSO for at least 1 hr. After that, new signals can be seen in the ^{1}H-NMR spectrum (< 1%), which can be attributed to the decomposition or transformation of the compound by ligand exchange with DMSO [29].

In vitro evaluation in synovial sarcoma cells

The photocytotoxicity (after irradiation) and cytotoxicity in the dark of photosensitizers **P1**-**P8** were evaluated *in vitro* on SW982 synovial sarcoma cells. A red-light lamp (λ = 630 nm) was used for irradiation (dose = 40 mW/cm^2 for 30 min). We decided to use red light because it is the only visible radiation that can pass through the skin and tissues of the synovial area of the joints. Blue radiation penetrates the skin for approximately 1 mm, green for about 2.5 mm, yellow not more than 4 mm, and red can penetrate as much as 5 mm before being fully absorbed [56]. The thickness of the human skin varies depending on the location between 0,5 - 4 mm, so to adapt our study to the future least invasive conditions possible, that is, transcutaneous PDT (without incision), irradiation with red light was the most appropriate.

Cell viability was analyzed by MTT assays for both, irradiated and non-irradiated cells. The results are shown in Table 1. The irradiated cells curve was fitted to the second order polynomial and from the resulting equation the IC_{50} (inhibitory concentration at 50% viability) was calculated (Fig. 5). All PSs showed good photocytotoxic activity after irradiation and no significant toxicity in the dark. The synthesized PSs present three structural variations. One of them is the arene ligand, which is *p*-cymene or phenylpropanol. Interestingly, the four PSs with PhPrOH groups (**P2**, **P4**, **P6** and **P8**) improve the result when compared to their *p*-cymene analogues (**P1**, **P3**, **P5** and **P7**) (Table 1). The higher activity might be attributed to the presence of OH groups, which can help to increase the production of ROS after irradiation, either by direct interaction with another excited PS molecules or

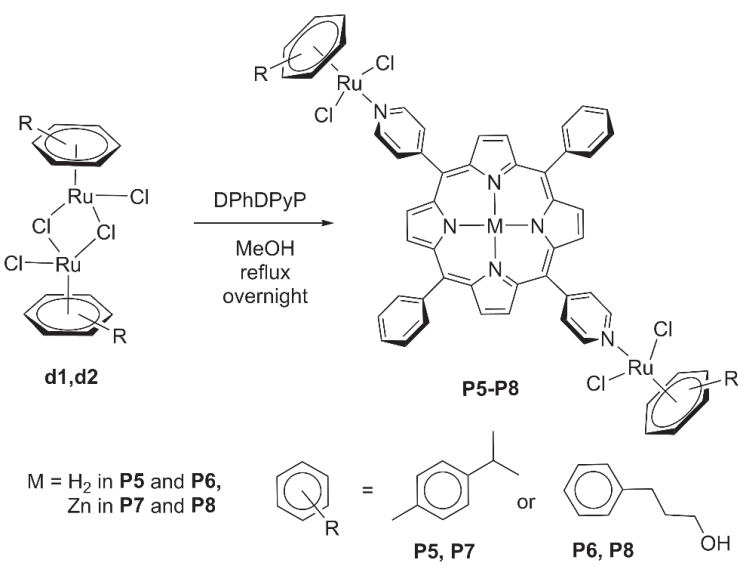

Scheme 2. Synthesis of photosensitizers **P5**-**P8** from dimers **d1** and **d2**.

Table 1. Results of MTT assays in synovial sarcoma cells after PDT. Graphic representations are shown in the supporting information (Fig. S48-S55). Irradiation 24 hr after addition of PS, $\lambda = 630$ nm, 40 mW/cm^2 for 30 min irradiation. IC_{50} was calculated fitting the curve to the second-degree polynomial ± 3 sigma deviation. The maximum concentration tested was 5 μM.

PS	Arene	Porphyrin	IC_{50} (μM) light	IC_{50} (μM) dark
P1	*p*-cymene	TPyP	0.170 ± 0.008	> 5
P2	PhPrOH	TPyP	0.060 ± 0.012	> 5
P3	*p*-cymene	Zn-TPyP	0.341 ± 0.008	1.092 ± 0.004
P4	PhPrOH	Zn-TPyP	0.256 ± 0.010	0.729 ± 0.005
P5	*p*-cymene	DPhDPyP	0.307 ± 0.014	> 5
P6	PhPrOH	DPhDPyP	0.212 ± 0.008	2.341 ± 0.005
P7	*p*-cymene	Zn-DPhDPyP	0.387 ± 0.010	1.096 ± 0.003
P8	PhPrOH	Zn-DPhDPyP	0.312 ± 0.010	0.689 ± 0.007

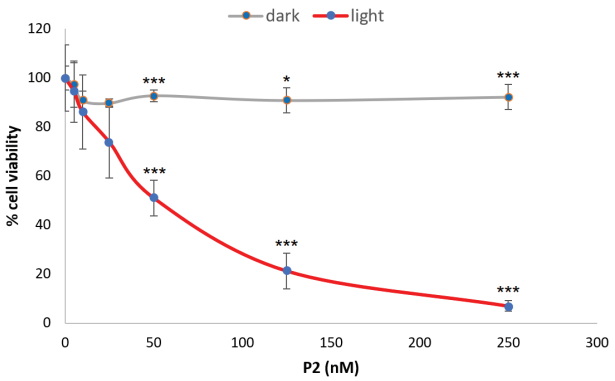

Fig. 5. Data obtained in the MTT assays in SW982 synovial sarcoma using **P2** as PS. Irradiation 24 hr after addition of **P2** (630 nm, 40 mW/cm^2, 30 min irradiation). Two-tailed Student's t-test significance, $P < 0.05$ (*), $P < 0.01$ (**) and $P < 0.001$ (***).

with other reactive species. Alcohols have been reported as an initial product in the production of ROS by metabolism [57]. In addition, porphyrins with phenol groups have proven their efficacy in PDT [58], as is the case of 5,10,15,20-tetra(*m*-hydroxyphenyl)chlorin (FOSCAN) [59–61]. Therefore, introduction of aliphatic alcohol at the periphery of a photosensitizer appears to be beneficial in our systems, increasing the PDT efficacy.

Another structural difference in **P1**-**P8** is the presence or absence of zinc in the center of the porphyrin. According to the results (Table 1), the presence of zinc worsens PDT efficacy. In all cases, the metal-free derivative shows a higher activity than its zinc analogue. One possible cause could be the fluorescence quantum yield ($Ø_F$). For instance, the photosensitizer **P1** shows a quantum yield lower than **P3** ($Ø_F^{P1}$ (%) = 3.0 and $Ø_F^{P3}$ (%) = 4.9) and the toxicity in the PDT of the first was higher. Fluorescence is a consequence of the energetic decay from the excited state of the PS to the minimum energy state. Therefore, high $Ø_F$ suggests that much of the energy in the singlet excited state of the PS returns to the ground state without passing through the triplet excited state, generating more fluorescence but leaving behind less energy in the triplet state to interact with O_2 and to give rise to ROS [62]. Zinc is responsible for this increased fluorescence. The fluorescence emission of PS containing zinc as a metal center is higher than the metal-free analogue (Fig. 6). This can also be understood from the point of view of the HOMO and LUMO orbitals. When the chromophore is excited, an electron rises from the highest energy occupied orbital (HOMO) to the lowest energy unoccupied orbital (LUMO). In the case that there is no metal center in the porphyrin, the electron vacancy that remains in the HOMO orbital can be filled by the lone pair electrons of the N in the tetrapyrrole unit. Then, the excited electron in the LUMO orbital will have more difficulties to return back to the HOMO orbital during relaxation, favoring intersystem crossing (see Fig. 2). On the other hand, if the porphyrin has a metal center coordinated to the N atoms of the tetrapyrrole through their lone pair electrons, the vacancy left in the HOMO orbital is not filled and the excited electron can return from the LUMO orbital easily, thus favoring fluorescence [63]. This may

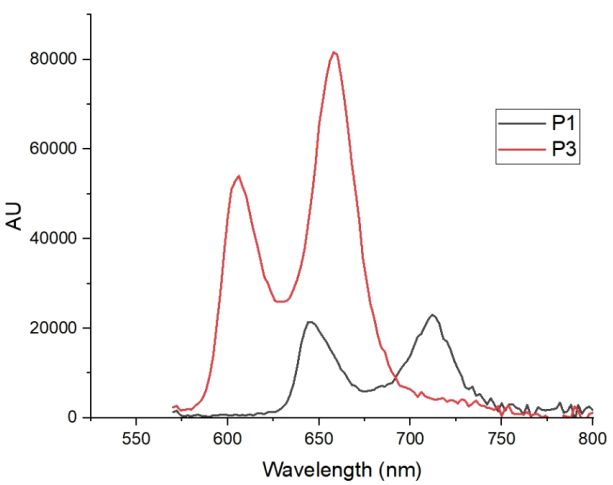

Fig. 6. Fluorescence spectrum of **P1** and **P3** (10 nM in DMSO).

explain why all our zinc-free PSs have a better IC_{50} under light than their zinc analogs.

The last structural difference in our PSs is the presence of two (DPhDPyP) or four (TPyP) pyridyl substituents on the PS and as a consequence, the presence of two or four coordinated arene ruthenium units. All PSs with DPhDPyP showed a reduced PDT effect than their tetranuclear counterparts. The reason may be due to the fact that PSs with DPhDPyP only have two coordinated ruthenium arenes, instead of the four presented in PSs with TPyP. Arene ruthenium complexes have been reported to improve solubility in biological media [45], thus potentially increasing uptake. Finally, it is worth noting the absence or very low toxicity of the compounds without metal (**P1**-**P4**) even at the highest concentration tested. While, Zn compounds (**P5**-**P6**) show some toxicity in the dark (Table 1). Similar results have been reported with zinc porphyrins, pointing to the metal as the cause for the cell growth decay [64, 65].

CONCLUSIONS

We report the synthesis and characterization of eight arene ruthenium porphyrin photosensitizers with great potential to treat synovial sarcoma by PDT. The photosensitizer **P2** showed the best light/dark photocytotoxicity ratio (0.06 μM/5 μM), being around two orders of magnitude. We have demonstrated that the presence of zinc (II) in the core of the photosensitizers have a double negative effect, increasing toxicity and reducing PDT efficacy. On the other hand, we have shown how alkyl alcohols on the arene ligands can improve the PDT effect in SW982 sarcoma cells. These results encourage us to continue studying these compounds and their potential in PDT, such as intracellular localization, PDT effect in another type of cancers, as well as performing an *in vivo* study.

EXPERIMENTAL

General

Compounds **d1**, **d2** and **P1** were prepared as described in the literature [47, 48, 42]. Methanol, ethanol, diethyl ether and deuterated solvents ($CDCl_3$ and DMSO-d_6) were acquired from Sigma-Aldrich and used as received. NMR spectra were recorded on a Bruker Avance III HD 500 MHz, Avance III HD 400 MHz or a DRX 400 MHz spectrometers. The ^1H and ^{13}C resonances of the deuterated solvents were used as the internal reference. Ruthenium(III) chloride hydrate, 1-isopropyl-4-methylcyclohexa-1,4-diene, 5,10,15,20-tetra(4-pyridyl)-21*H*,23*H*-porphine and zinc 5,10,15,20-tetra(4-pyridyl)-21*H*,23*H*-porphine were acquired from Sigma-Aldrich, 3-(cyclohexa-1,4-dien-1-yl)propan-1-ol from Fisher Scientific and 5,15-diphenyl-10,20-di(pyridin-4-yl)porphyrin and zinc 5,15-diphenyl-10,20-di(pyridin-4-yl)porphyrin from Porphychem. We carried out all the *in vitro* tests and manipulations under an aseptic atmosphere and constant sterilization conditions. SW982 sarcoma synovial cells were provided by the American Type Culture Collection (ATCC—LGC Standards). Cells were grown in DMEM medium supplemented with 10% fetal bovine serum, 1% L-glutamine and 100 U/ml penicillin and 100 μg/ml streptomycin (Gibco BRL, Cergy-Pontoise, France). 3-(4,5-Dimethylthiazol-2-yl)-2,5-diphenyltetrazolium bromide (MTT) and L-glutamine were acquired from Sigma-Aldrich. Dimethyl sulfoxide (DMSO) was bought in Acros Organics. The PSs (**P1**-**P8**) were dissolved at 1 mM concentration in DMSO just before use, then diluted in complete medium to the needed concentration and immediately preceding to use. The concentration of DMSO in the cell medium was in all cases lower than 0.25%. Cell irradiation was carried out using a red-light source, CureLight®, PhotoCure ASA, at 630 nm, and dose 40 mW/cm^2 for 30 min. Absorbance after MTT assay was measured at 540 nm by a Dynex Triad Multi Mode Microplate Reader, Dynex Technologies. UV-vis spectrums were carried out in SI Analytics model UvLine 9400 (Xenon lamp) spectrophotometer, 1.5 mL polystyrene cuvettes (wavelength range 280–800 nm) and diluting the PS in DMSO (10 nM). Fluorescence spectra were measured (550–800 nm) on a FLS980 spectrometer from Edinburgh Instruments, using 5,10,15,20-tetraphenylporphin as reference in toluene, while the PSs were dissolved 10 nM in DMSO. IR spectra were performed on a Frontier PerkinElmer spectrometer (600 – 4000 cm^{-1}). Spectra are shown in the Supporting Information (Fig. S1-S47).

Photocytotoxicity evaluation by MTT assays

First, trypsinization and counting of SW982 synovial sarcoma cells were carried out. Homogeneous solutions were prepared in 10 mL of culture medium with 700,000 cells. In a 96-well plate, 100 μL of the solution (7000 cells per well) were poured and the cells were incubated for 24 hr (37 °C and 5% CO_2). After that, 100 μL of PS solution in increasing concentration were poured per row in the plate and subsequent incubation 24 hr in the same conditions previously described. The PSs were dissolved in DMSO just before use and then added to culture medium in the desired concentrations. We have decided to use DMSO since it is the only solvent in which all PSs showed acceptable solubility, to keep the same experimental conditions. After incubation the medium was removed carefully and poured 100 μL of complete medium without red phenol per well. Then, the activation of PS by irradiation with red light (λ = 630 nm) is then carried out, applying 40 mW/cm^2 for 30 min. The lamp is put at 12 cm above of the plate in vertical position. After the irradiation the 96-well plate was put in the incubator during 18 hr. After this time, we added 10 μL of MTT solution (5 g/L) and the plate was put again inside the

incubator during 4 hr. Then, the media was removed and added 200 µL of DMSO per well, stirring the plate gently (to avoid splashing between wells) for 3 min until homogenized. Finally, the absorbance was measured at 550 nm. This whole process was repeated in triplicate. Cytotoxicity measurements in the absence of light were carried out by repeating this entire protocol except the irradiation dose. The results obtained in the photocytotoxicity tests were expressed graphically as the mean ± three standard deviations. Statistical significance was calculated using the Student's t-test where $P < 0.05$, < 0.01 and < 0.001 is expressed as *, ** and *** respectively.

***Synthesis of P2*.** In a 100 mL round bottom flask, a solution containing 60.0 mg (0.098 mml) of **d2** and 30.1 mg (0.049 mmol) of TPyP in 30 mL of MeOH, was prepared. The solution was refluxed for 12 hr, then cooled to room temperature. The solution was filtered off and the resulting brown solid was washed with Et_2O (5 × 10 mL).

***P2*.** Yield 86% (78 mg). ^{1}H NMR (DMSO-d_6, 25 °C, 500 MHz): δ 9.08 (m, 8H, CH_{py}), 8.92 (br s, 8H, CH_{porph}), 8.28 (m, 8H, CH_{py}), 5.98 (m, 8H, *m*-CH_{ar}), 5.76 (overlapping doublets, 8H, *o*-CH_{ar}), 5.75 (overlapping triplets, 4H, *p*-CH_{ar}), 4.59 (s, 4H, O*H*), 3.45 (m, 8H, CH_2), 2.47 (m, 8H, CH_2), 1.73 (m, 8H, CH_2), -3.06 (s, 2H, N*H*). ^{13}C NMR (DMSO-d_6, 25 °C, 125 MHz): δ 142.06 (C_{py}), 128.16 (C_{py}), 128.10 (C_{porph}), 125.46 (C_{py}), 107.83 ($C_{propanol}$), 88.79 (*m*-C_{ar}), 84.80 (*o*-C_{ar}), 82.91 (*p*-C_{ar}), 59.89 (*C*H$_2$), 32.04 (*C*H$_2$), 29.42 (*C*H$_2$). UV/vis (DMSO), λ, nm (ε, $M^{-1}.cm^{-1}$): 445 (262300), 523 (197400), 588 (152500), 638 (125300). FT-IR (ATR, solid, cm^{-1}): ν; br s (3700-3200), s (3108), s (2916), s (2824), s (1614), s (1418).

The synthesis of **P3** and **P4** utilize the same protocol and molar ratio as in **P2**, but using the corresponding dimer (**d1**, **d2**) and porphyrin. **P5-P8** are synthesize in the same manner but using a molar ratio of 1:1 (dimer:porphyrin) (**DPhDPyP** or **Zn-DPhDPyP**).

***P3*.** Yield 81% (234 mg). ^{1}H NMR (DMSO-d_6, 25 °C, 400 MHz): δ 9.03 (d, $^3J_{HH}$ = 5.55 Hz, 8H, CH_{py}), 8.85 (s, 8H, CH_{porph}), 8.23 (d, $^3J_{HH}$ = 5.72 Hz, 8H, CH_{py}), 5.83 (d, $^3J_{HH}$ = 6.14 Hz, 8H, CH_{ar}), 5.78 (d, $^3J_{HH}$ = 6.15 Hz, 8H, CH_{ar}), 2.84 (m, $^3J_{HH}$ = 6.91 Hz, 4H, CH_{iPr}), 4.58 (bs, 4H, O*H*), 2.09 (s, 12H, CH_3), 1.20 (m, $^3J_{HH}$ = 5.55 Hz, 24H, C$H_{3\ iPr}$). ^{13}C NMR (DMSO-d_6, 25 °C, 101 MHz): δ 149.12 (C_{ar}), 148.50 (C_{py}), 132.48 (C_{porph}), 129.72 (C_{py}), 118.57 (C_{py}), 106.83 (C_{porph}), 100.56 (C_{ar}), 86.83 (*C*H$_{ar}$), 85.99 (*C*H$_{ar}$), 30.44 (*C*H$_{iPr}$), 21.97 (*C*H$_{3\ iPr}$), 18.34 (*C*H$_3$). Elemental analysis: Calcd. for $C_{80}H_{80}Cl_8N_8O_4Ru_4Zn$ + 4 H_2O: C, 48.56; H, 4.48; N 5.66. Found: C, 48.46; H, 4.63; N, 5.90. UV/vis (DMSO), λ, nm (ε, $M^{-1}.cm^{-1}$): 472 (59400), 518 (138300), 558 (55000), 599 (53300). FT-IR (ATR, solid, cm^{-1}): ν; br s (3600-3250), s (3091), s (2944), s (2881), s (1609).

***P4*.** Yield 88% (82 mg). ^{1}H NMR (DMSO-d_6, 25 °C, 400 MHz): δ 9.02 (br s, 8H, CH_{py}), 8.65 (br s, 8H, CH_{porph}), 8.22 (br s, 8H, CH_{py}), 5.98 (m, 8H, *m*-CH_{ar}), 5.75 (overlapping doublet, 8H, *o*-CH_{ar}), 5.73 (overlapping triplet, 4H, *p*-CH_{ar}), 4.58 (br s, 4H, O*H*), 3.45 (m, 8H, CH_2), 2.48 (m, 8H, CH_2), 1.73 (m, 8H, CH_2). ^{13}C NMR (DMSO-d_6, 25 °C, 101 MHz): δ 149.11 (C_{ar}), 148.47 (C_{py}), 132.48 (C_{porph}), 129.72 (C_{py}), 108.44 ($C_{propanol}$), 89.40 (*m*-C_{ar}), 85.33 (*o*-C_{ar}), 83.43 (*p*-C_{ar}), 60.46 (*C*H$_2$), 32.64 (*C*H$_2$), 30.00 (*C*H$_2$). Elemental analysis: Calcd. for $C_{76}H_{72}Cl_8N_8O_4Ru_4Zn$: C, 47.67; H, 3.79; N 5.85. Found: C, 47.67; H 3.79; N 6.09. ESI-MS, m/z, 954.8 [M – [Ru(PhPrOH)-$Cl_2]_3$ – Cl]$^{+1}$. UV/vis (DMSO), λ, nm (ε, $M^{-1}.cm^{-1}$): 522 (95300), 561 (45200), 598 (49800). FT-IR (ATR, solid, cm^{-1}): ν; br s (3500-3200), s (3067), s (2910), s (2881), s (1619), s (1408).

***P5*.** Yield 51% (51 mg). ^{1}H NMR ($CDCl_3$, 25 °C, 400 MHz): δ 9.47 (m, 4H, CH_{py}), 8.87 (m, 10H, CH_{Ph}), 8.21 (m, 8H, CH_{porph} and CH_{py}), 7.78 (br s, 4H, CH_{porph}), 5.69 (d, $^3J_{HH}$ = 5.72 Hz, 4H, CH_{ar}), 5.47 (d, $^3J_{HH}$ = 5.48 Hz, 4H, CH_{ar}), 3.20 (m, 2H, CH_{iPr}), 2.23 (s, 6H, CH_3), 1.47 (d, $^3J_{HH}$ = 6.86 Hz, 12H, C$H_{3\ iPr}$), -2.81 (s, 1H, N*H*), -2.87 (s, 1H, N*H*). ^{13}C NMR ($CDCl_3$, 25 °C, 101 MHz): δ 153.04 (C_{py}), 141.76 (C_{ph}), 134.54 (C_{py}), 130.20 (C_{ph}), 127.97 (C_{py}), 126.77 (C_{porph}), 121.55 (C_{porph}), 120.93 (C_{porph}), 83.23 (*C*H$_{ar}$), 82.55 (*C*H$_{ar}$), 30.92 (*C*H$_{iPr}$), 22.50 (*C*H$_{3\ iPr}$), 18.42 (*C*H$_3$). Elemental analysis: Calcd. for $C_{62}H_{56}Cl_4N_6Ru_2$: C, 60.99; H, 4.59; N 6.84. Found: C, 62.76; H 4.81; N 7.09. UV/vis (DMSO), λ, nm (ε, $M^{-1}.cm^{-1}$): 513 (143500), 549 (319100), 590 (134400), 648 (29000). FT-IR (ATR, solid, cm^{-1}): ν; br s (3550-3400), s (3080), s (2968), s (1638), s (1491).

***P6*.** Yield 61% (60 mg). ^{1}H NMR ($CDCl_3$, 25 °C, 400 MHz): δ 9.50 (d, $^3J_{HH}$ = 5.96 Hz, 4H, CH_{py}), 8.89 (m, 10H, CH_{Ph}), 8.23 (m, 8H, CH_{porph} and CH_{py}), 7.80 (m, 4H, CH_{porph}), 5.93 (t, $^3J_{HH}$ = 5.64 Hz, 4H, *m*-CH_{ar}), 5.81 (t, $^3J_{HH}$ = 5.58 Hz, 2H, *p*-CH_{ar}), 5.62 (d, $^3J_{HH}$ = 5.72 Hz, 4H, *o*-CH_{ar}), 3.88 (q, $^3J_{HH}$ = 5.83 Hz, 4H, CH_2), 2.84 (t, $^3J_{HH}$ = 7.71 Hz, 4H, CH_2), 2.07 (m, 4H, CH_2), 1.69 (overlapping multiplet, 2H, O*H*), -2.80 (s, 2H, N*H*). Elemental analysis: Calcd. for $C_{60}H_{52}Cl_4N_6O_2Ru_2$: C, 58.45; H, 4.25; N 6.82. Found: C, 59.85; H 4.56; N 6.88. UV/vis (DMSO), λ, nm (ε, $M^{-1}.cm^{-1}$): 509 (43400), 550 (154700), 589 (48200), 648 (4000). FT-IR (ATR, solid, cm^{-1}): ν; br s (3600-3200), s (3102), s (2892), s (1641).

***P7*.** Yield 54% (68 mg). ^{1}H NMR (DMSO-d_6, 25 °C, 400 MHz): δ 9.00 (m, 4H, CH_{py}), 8.82 (m, 10H, CH_{Ph}), 8.20 (m, 8H, CH_{porph} and CH_{py}), 7.81 (m, 4H, CH_{porph}), 5.83 (d, $^3J_{HH}$ = 5.39 Hz, 4H, CH_{ar}), 5.78 (d, $^3J_{HH}$ = 6.18 Hz, 4H, CH_{ar}), 2.84 (m, 2H, CH_{iPr}), 2.09 (s, 6H, CH_3), 1.20 (d, $^3J_{HH}$ = 6.94 Hz, 12H, C$H_{3\ iPr}$). Elemental analysis: Calcd. for $C_{62}H_{54}Cl_4N_6Ru_2Zn$: C, 57.62; H, 4.21; N 6.50. Found: C, 58.51; H 4.32; N 6.59. ESI-MS, m/z, 950.9 [M – [Ru(*p*-cymene)Cl_2] – Cl]$^{+1}$, 680.8 [Zn-DPhDPyP + H]$^{+1}$. UV/vis (DMSO), λ, nm (ε, $M^{-1}.cm^{-1}$): 493 (55600), 524 (99900), 562 (349500), 600 (221100), 626 (81300) (. FT-IR (ATR, solid, cm^{-1}): ν; br s (3650-3200), s (3080), s (2988), s (1639).

***P8*.** Yield 67% (84 mg). ^{1}H NMR (DMSO-d_6, 25 °C, 400 MHz): δ 9.01 (m, 4H, CH_{py}), 8.82 (m, 10H, CH_{Ph}), 8.20 (m, 8H, CH_{porph} and CH_{py}), 7.82 (m, 4H, CH_{porph}),

5.99 (m, 4H, *m*-CH_{ar}), 5.75 (m, 6H, *p*-CH_{ar} and *o*-CH_{ar}), 4.59 (m, 2H, O*H*), 3.46 (m, 4H, CH_2), 2.47 (m, 4H, CH_2), 1.73 (m, 4H, CH_2). Elemental analysis: Calcd. for $C_{60}H_{50}Cl_4N_6O_2Ru_2Zn$: C, 55.59; H, 3.89; N 6.48. Found: C, 56.44; H 4.09; N 6.56. ESI-MS, m/z, 952.9 $[M - [Ru(PhPrOH)Cl_2] - Cl]^{+1}$. UV/vis (DMSO), λ, nm (ε, $M^{-1}.cm^{-1}$): 482 (21700), 521 (46900), 559 (253400), 600 (108700), 626 (37900). FT-IR (ATR, solid, cm^{-1}): ν; br s (3580-3150), s (3012), s (2917), s (1591).

Acknowledgments

We thank all the people involved in the project POLYTHEA, funding by European Union's Horizon 2020 under the Marie Sklodowska-Curie grant agreement no. 764837. M. G.-V. thanks Stéphanie Leroy-Lhez, Johann Bouclé and Nidia Maldonado-Carmona for access to fluorescence equipment and for their great help.

Supporting information

Additional photosensitizer results are given in the supplementary material. This material is available free of charge *via* the Internet at https://www.worldscientific.com/doi/suppl/10.1142/S1088424622500018

REFERENCES

1. Dougherty TJ, Gomer CJ, Henderson BW, Jori G, Kessel D, Korbelik MJ and Peng Q. *J. Natl Cancer Inst.* 1998; **90**: 889–905.
2. Dolmans DE., Fukumura D and Jain RK. *Nat. Rev. Cancer*. 2003; **3**: 380–387.
3. De Silva P, Saad MA, Thomsen HC, Bano S, Ashraf S and Hasan T. *J Porphyrins Phthalocyanines*. 2020; **24**: 1320–1360.
4. Vargas-Zúñiga GI, Kim HS, Li M, Sessler JL and Kim JS. *J Porphyrins Phthalocyanines*. 2021; **25**: 773–793.
5. Mroz P, Yaroslavsky A, Kharkwal GB and Hamblin MR. *Cancers*. 2011; **3**: 2516–2539.
6. Buytaert E, Dewaele M and Agostinis P. *BBA-Rev Cancer*. 2007; **1776**: 86–107.
7. Simon HU, Haj-Yehia A and Levi-Schaffer F. *Apoptosis*. 2000; **5**: 415–418.
8. Dos Santos AF, De Almeida DRQ, Terra LF, Baptista MS and Labriola, L. *J Cancer Metastasis Treat*. 2019; **5**: 25.
9. Zhang L, Ji Z, Zhang J and Yang S. *Photodiagnosis Photodyn Ther*. 2019; **28**: 159–165.
10. Hilerowicz Y, Friedman O, Zur E, Ziv R, Koren A, Salameh F, Mehrabi JN and Artzi O. *Lasers Surg Med*. 2020; **52**: 966–970.
11. Ding HL, Wang XL, Wang HW and Huang Z. *Photodiagnosis Photodyn Ther*. 2011; **8**: 343–346.
12. Ruiz-Moreno JM, Montero JA and Barile S. *Eur. J. Ophthalmol*. 2006; **16**: 426–434.
13. Montero JA, Ruiz-Moreno JM and Fernandez-Muñoz M. *Eur J Ophthalmol*. 2011; **21**: 503–505.
14. Kusuzaki K, Murata H, Matsubara T, Miyazaki S, Shintani K, Seto M, Matsumine A, Hosol A, Sugimoto T and Uchida A. *Photochem Photobiol*. 2005; **81**: 705–710.
15. Takeda K, Kunisada T, Miyazawa S, Nakae Y and Ozaki T. Clinical orthopaedics and related research. 2008; **466**: 1726–1733.
16. Gallardo-Villagrán M, Leger DY, Liagre B, Therrien B. *Int J Mol Sci*. 2019; **20**: 3339.
17. Maisch T, Szeimies RM, Jori G and Abels C. *Photochem. Photobiol. Sci*. 2004; **3**: 907–917.
18. Maldonado-Carmona N, Ouk TS, Calvete MJ, Pereira MM, Villandier N and Leroy-Lhez S. *Photochem. Photobiol. Sci*. 2020; **19**: 445–461.
19. Siegel, H. J., Sessions, W., Casillas Jr, M. A., Said-Al-Naief, N., Lander, P. H. and Lopez-Ben, R. *Orthopedics*. 2007; **30**: 1020.
20. Cadman NL, Soule EH and Kelly PJ. 1965; **18**: 613–627.
21. Bergovec M, Smerdelj M, Bacan F, Seiwerth S, Herceg D and Prutki M. *Orthop Traumatol Surg Res.* 2018; **104**: 227–230.
22. Kampe CE, Rosen G, Eilber F, Eckardt J, Lowenbraun S, Foster J, Forscher C and Selch M. *Cancer*. 1993; **72**: 2161–2169.
23. Gunaydin G, Gedik ME and Ayan S. *Front Chem*. 2021; **9**: 400.
24. Lucky SS, Soo KC and Zhang Y. *Chem Rev*. 2015; **115**: 1990–2042.
25. Jiang Z, Shao J, Yang T, Wang J and Jia L. *J Pharm Biomed Anal*. 2014, **87**: 98–104.
26. Huang H, Yu B, Zhang P, Huang J, Chen Y, Gasser G, Ji L and Chao H. *Angew Chem Int Ed*. 2015; **54**: 14049–14052.
27. Dubuc C, Langlois R, Bénard F, Cauchon N, Klarskov K, Tone P and van Lier JE. *Bioorg Med Chem Lett*. 2008; **18**: 2424–2427.
28. Liang G, Wang L, Yang Z, Koon H, Mak N, Chang CK and Xu B. *Chem Comm*. 2006; **48**: 5021–5023.
29. Patra M, Joshi T, Pierroz V, Ingram K, Kaiser M, Ferrari S, Spingler B, Keiser J and Gasser G. *Chem Eur J*. 2013; **19**: 14768–14772.
30. Roy I, Bobbala S, Young RM, Beldjoudi Y, Nguyen MT, Cetin MM, Cooper JA, Allen S, Anamimoghadam O, Scott EA, Wasielewski MR and Stoddart JF. *J Am Chem Soc*. 2019; **141**: 12296–12304.
31. Leonidova A, Anstaett P, Pierroz V, Mari C, Spingler B, Ferrari S and Gasser G. *Inorg Chem*. 2015; **54**: 9740–9748.
32. Leonidova A, Mari C, Aebersold C and Gasser G. *Organometallics*. 2016; **35**: 851–854.
33. Hockel M and Vaupel P. *J Natl Cancer Inst*. 2001; **93**: 266–276.
34. Vaupel P, Mayer A and Höckel M. *Methods Enzymol*. 2004; **381**: 335–354.

35. Maier A, Tomaselli F, Anegg U, Rehak P, Fell B, Luznik S, Pinter H and Smolle-Jüttner FM. *Eur J Cardiothorac Surg*. 2000; **18**: 649–655.
36. Bonnett R, Djelal BD and Nguyen A. *J Porphyrins Phthalocyanines*. 2001; **5**: 652–661.
37. Kaspler P, Lazic S, Forward S, Arenas Y, Mandel A and Lilge L. *Photochem Photobiol Sci*. 2016; **15**: 481–495.
38. Lv Z, Wei H, Li Q, Su X, Liu S, Zhang KY, Lv W, Zhao Q, Li X and Huang W. *Chem Sci*. 2018; **9**: 502–512.
39. Yano T, Hishida S, Nakai M and Nakabayashi Y. *Inorganica Chim Acta*. 2017; **454**: 162–170.
40. Lei W, Zhou Q, Jiang G, Zhang B and Wang X. *Photochem Photobiol Sci*. 2011; **10**: 887–890.
41. Huang H, Zhang P, Yu B, Jin C, Ji L and Chao H. *Dalton Trans*. 2015; **44**: 17335–17345.
42. Schmitt F, Govindaswamy P, Süss-Fink G, Ang WH, Dyson PJ, Juillerat-Jeanneret L and Therrien B. *J Med Chem*. 2008; **51**: 1811–1816.
43. Schmitt F, Freudenreich J, Barry NP, Juillerat-Jeanneret L, Süss-Fink G and Therrien B. *J Am Chem Soc*. 2012; **134**: 754–757.
44. Therrien B and Furrer J. *Adv Chem Eng*. 2014; **2014**: 1–20.
45. Yano T, Hishida S, Nakai M and Nakabayashi Y. *Inorganica Chim Acta*. 2017; **454**: 162–170.
46. Bogoeva V, Siksjø M, Sæterbø KG, Melø TB, Bjørkøy A, Lindgren M and Gederaas OA. *Photodiagn Photodyn Ther*. 2016; **14**: 9–17.
47. Zelonka RA and Baird M. *Can J Chem*. 1972; **50**: 3063–3072.
48. Čubrilo J, Hartenbach I, Schleid T and Winter RF. *Z Anorg Allg Chem*. 2006; **632**: 400–408.
49. Govindaswamy P, Süss-Fink G and Therrien B. *Organometallics*. 2007; **26**: 915–924.
50. Stringer T, Therrien B, Hendricks DT, Guzgay H and Smith GS. *Inorg Chem Commun*. 2011; **14**: 956–960.
51. Gupta G, Yap GP, Therrien B and Rao KM. *Polyhedron*. 2009; **28**: 844–850.
52. Kota TP and Kollipara MR. *J Chem Sci*. 2014; **126**: 1143–1151.
53. Schmitt F, Govindaswamy P, Süss-Fink G, Ang WH, Dyson PJ, Juillerat-Jeanneret L and Therrien B. *J Med Chem*. 2008; **51**: 1811–1816.
54. Villarroel A, Duff A and Hu T. *FASEB J*. 2020; **34**: 1–1.
55. Nguyen ST, Nguyen HTL and Truong KD. *Biomed Res Ther*. 2020; **7**: 3855–3859.
56. Clement M, Daniel G and Trelles M. *J Cosmet Laser Ther*. 2005; **7**: 177–189.
57. Gomes AC, Mello AL, Ribeiro MG, Garcia DG, Da Fonseca CO, Salazar MDA, Schönthal AH and Quirico-Santos T. *Arch Immunol Ther Exp*. 2017; **65**: 285–297.
58. Mroz P, Bhaumik J, Dogutan DK, Aly Z, Kamal Z, Khalid L, Kee HL, Bocian DF, Holten D, Lindsey JS and Hamblin MR. *Cancer lett*. 2009; **282**: 63–76.
59. Jones HJ, Vernon DI and Brown SB. *Br J Cancer*. 2003; **89**: 398–404.
60. Meier D, Botter SM, Campanile C, Robl B, Gräfe S, Pellegrini G, Born W and Fuchs B. *Int J Cancer*. 2017; **140**: 1680–1692.
61. Senge MO and Brandt JC. *Photochem Photobiol*. 2011; **87**: 1240–1296.
62. Kamkaew A, Lim SH, Lee HB, Kiew LV, Chung LY and Burgess K. *Chem Soc Rev*. 2013; **42**: 77–88.
63. Afaneh AT and Schreckenbach G. *Am J Phys Chem*. 2015; **119**: 8106–8116.
64. Lutton JD, Abraham NG, Drummond GS, Levere RD and Kappas A. *Proc Natl Acad Sci*. 1997, **94**: 1432–1436.
65. Yang G, Nguyen X, Ou J, Rekulapelli P, Stevenson DK and Dennery PA. *Am J Hematol*. 2001; **97**: 1306–1313.